OpenFOAM Simulation and Experimental Analysis of the Influence of Geometric Parameters of Heat Sinks on Natural Convection

Silva, V. A., Neves Gomes, L. A. C., Lima e Silva, A. L. F. and Lima e Silva, S. M. M.
Heat Transfer Laboratory – LabTC,
Mechanical Engineering Institute - IEM,
Federal University of Itajubá - UNIFEI,
Av. BPS, 1303, Itajubá, MG, Brazil
E-mail: altairwayne@gmail.com, gomeslorenzo@gmail.com, alfsilva@unifei.edu.br, metrevel@unifei.edu.br

ABSTRACT

In the present work, the unsteady and steady state heat transfer by natural convection in heat sinks, horizontally oriented, with flat and rectangular fins was studied. For that, the free and open source CFD software OpenFOAM (Open Field Operation and Manipulation) was used to solve the three-dimensional equations of continuity, momentum and energy. The Finite Volume Method for the discretization of the governing equations and the PIMPLE solution algorithm for the pressure-velocity coupling were used. The temperature, velocity and vorticity fields were numerically obtained. Experiments were also carried out to validate the computational studies. Two 6063-T5 aluminum heat sinks were studied. In addition, analyses were realized in the relation between the power provided and the temperature that has been achieved by the heat sink. Through this relation, the heat sinks can be classified and identified according to their capacity to dissipate heat. The values of the average convection heat transfer coefficient and the Nusselt number, numerically obtained, were compared with the experimental values. These results obtained were in accordance with the empirical correlation found in literature, with average differences lower than 10%.

INTRODUCTION

The study of the process of natural and forced convection in finned plates [1] showed two effects: First, the position of the fin array, relative to the gravitational field in natural convection, and relative to a free stream in forced convection. Second, the effect of the tilting of the crests of the plate fins relative to the approaching flow. In each configuration, the results based on complete three-dimensional numerical simulations of the flow and heat transfer confirm the validity of the results determined based on direct measurements. In brief, the best plate fins are those with crests tilted such that their tops face the approaching flow. The augmentation effect associated with tilting the crests increases as the air flow increases, for example, in switching from natural to forced convection, or increasing Re_L in forced convection.

NOMENCLATURE

A	m²	Area
b	mm	Fin base Thickness
c_p	J/Kg.K	Specific Heat
ct	-	Cross fin section
$\vec{g}$	m/s²	Vector Acceleration of Gravity
h	W/m.K	Local Heat Transfer Coefficient by Free Convection
$\bar{h}$	W/m.K	Medium Heat Transfer Coefficient by Free Convection
H	m	Fin Height
$(H\&R)$	-	Harahap and Rudianto (2005) [6]
k	W/m.K	Thermal Conductivity
L	m	Heat sink lenght
n	-	Number of fin in Heat sink
Nu	-	Nusselt Number
s	mm	Fin Spacing
t	s	Time
t_w	mm	Thickness
T	K	Temperature
W	m	Fin Width

Special characters

α	m²/s	Thermal Diffusivity
Δ	-	Difference
μ	Pa.s	Dynamics Viscosity
ρ	kg/m³	Specific Mass
∂	-	Differential Operator
∇^2	m^{-2}	Laplacian Operator

Subscripts

x	-	Cartesian coordinate
y	-	Cartesian coordinate
z	-	Cartesian coordinate
0	-	Environmental
1	-	Thermocouple Position and Name
2	-	Thermocouple Position and Name
3	-	Thermocouple Position and Name
4	-	Thermocouple Position and Name
5	-	Thermocouple Position and Name
∞	-	Environment

Jouhara and Axcell [2] provided a comprehensive description of the thermal conditions within a heat sink with rectangular fins under conditions of cooling by laminar forced convection. The analysis, in which increasing complexity was progressively introduced, used both classical heat transfer theory and a computational approach to model the increase in air temperature through the channels formed by adjacent fins and the results agreed well with published experimental data.

Several analyses were performed by Silva *et al.* [3] and Silva [4] to determine the optimal number and position of the sensors used to measure the experimental temperature on the heat sinks. These analyses confirmed the uniformity of the temperature distribution on the heat sink surface. This allowed the use of thermocouples only in the center of the heat sink, which facilitates the experimental procedures. Furthermore, an analysis of the positions of the heat sink basis performed by Silva *et al.* [3] and Silva [4] point that the

vertical position in free convection is better than the horizontal. The same behavior was presented in Tari and Mehrtash [5] in their numerical investigation. They studied heat sinks in different positions by varying their angles from horizontal to vertical and downwards. This study focused on numerical simulations and on investigation of Nusselt and Rayleigh numbers. The objective of Tari and Mehrtash [5] was to propose correlations for Nusselt number by using the numerical simulations for heat sinks in vertical and in different angles by using the cosine as an adjustment parameter.

In this work, the main goal was to numerically study the heat transfer by free convection in heat sinks and to analyse the mass, pressure, velocity and temperature fields obtained through the use of the OpenFOAM software. The validation of the temperature, *h*, and *Nu* results was done by comparing experimental results and the empirical correlation of Harahap and Rudianto [6].

THEORETICAL BASIS

In this work, the problem studied is a solid plate subjected to heat transfer by conduction and natural convection. Therefore, the equations of conservation of mass, momentum and energy must be solved. This group of equations were numerically solved by the software OpenFOAM.

Modeling the Solid Medium

The heat flux determination in a section of the solid medium is only possible when the temperature gradient along this medium is known. This temperature gradient can be obtained by applying an energy balance in an appropriated differential control volume.

Considering constant thermophysical properties of the heat sink, the energy conservation can be expressed as:

$$\frac{\partial^2 T}{\partial x^2}(x,y,z,t)+\frac{\partial^2 T}{\partial y^2}(x,y,z,t)+\frac{\partial^2 T}{\partial z^2}(x,y,z,t)=\frac{1}{\alpha}\frac{\partial T}{\partial t}(x,y,z,t) \quad (1)$$

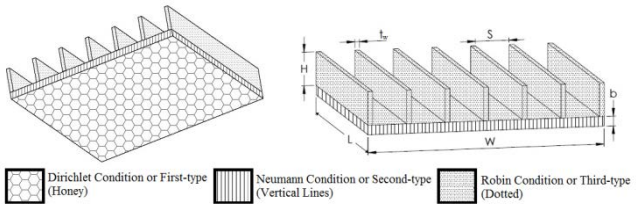

Figure 1 Representation of different domains and the geometric parameters of the heat sink.

Using the right boundary conditions, equation (1) can be used to determine the heat distribution in the heat sink. In this work, tree boundary conditions were used. The Dirichlet Condition (or first-type) specifies a temperature value; the Neumann Condition (or second-type) considers a heat flux on the heat sink boundary (even if it is a null heat flux, as in an adiabatic or isolated surface) and the Robin Condition (or third-type) which considers the heating or cooling of a surface by convection. Figure 1 shows the heat sink geometry and where the boundary conditions above described were applied and also presents the geometric parameters of the heat sink (*L*, *W*, and *H*). The boundary conditions can be expressed as:

- Constant temperature, T_5, in honey pattern area in Figure 1;
- Isolated Surface in vertical lines area in Figure 1;
- Cooling by free convection on surface in dotted area in Figure 1;

And the initial condition is:

$$T(x,y,z,0)=T_0 \quad (2)$$

Hereafter are described the equations used to model the fluid medium.

Modeling the Fluid Medium

When considering a compressible flow, disregarding the viscous dissipation and the internal generation as well as pressure variations, introducing Fourier's law, and considering a constant thermal conductivity the equation is as follows:

$$\frac{\partial T}{\partial t}+u\frac{\partial T}{\partial x}+v\frac{\partial T}{\partial y}+w\frac{\partial T}{\partial z}=\alpha\nabla^2 T \quad (3)$$

By considering the air as a Newtonian fluid and a constant viscosity flow, the momentum equation can be written as the simplified Navier-Stokes equation:

$$\rho\frac{\partial \vec{U}}{\partial t}=\rho\,\vec{g}-\vec{\nabla}\,p+\mu\nabla^2\vec{U} \quad (4)$$

The domain in this simulation is a 600 mm cube that represents the control volume used as the fluid medium [5]. The domain is about 43 times bigger than the heat sink height while the length and width are six times the respective dimensions of the heat sink.

The button surface of the domain has a condition of heat exchange by free convection with the heat sink and the wood board. Environmental temperature T_1 is imposed to all the lateral surfaces and to the top of the domain. The heating of the fluid happens by heat exchange with the heat sink, where temperature T_5 is imposed on its base.

When a closed domain is considered, the boundary conditions for the velocity are null in all surfaces, because all the areas in contact with the fluid present a null velocity. The pressure was adjusted according to the velocity conditions in all surfaces, while a condition of maximum pressure, equal to the atmospheric pressure, is imposed on the top surface.

COMPUTACIONAL MODELING OF THE PROPOSED PROBLEM

Pre-processing

The first step to study the proposed problem was the choice of the software. OpenFOAM was chosen because it is free and open source software. It has different tools of discretization in space and time and has its own mesh generator. The second step was to define a solver. The solver can be developed by the user or chosen among the available solvers. However, it must have the necessary equations to solve the problem and the relevant libraries as, for example, physical and thermodynamic proprieties. The chosen solver

was the *chtMultiRegionFoam*, which is appropriate to solve steady and unsteady state problems that involve heat transfer between fluid and solids.

The mesh used in all simulations has approximately six millions hexahedral elements. This mesh was chosen after conducting a mesh refinement test, summarized in Table 1. This test was carried out after the steady state was reached. Figure 2 presents 3 different views of the mesh used.

Table 1 – Mesh refinement test.

Mesh	Elements	Temperature	Simulation Time
I - 220x220xx80	3.5 Millions	310.8 K	24 hours
II - 2060x260x90	6 Millions	315.61 K	80 hours
III - 300x300x90	8 Millions	315.60 K	144 hours

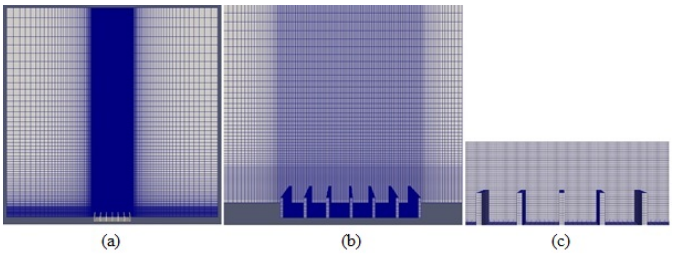

Figure 2 View of the computational mesh. (a) the whole domain, (b) view of the heat sink, and (c) view of the fins.

After defining the domain and informing the program which cells belongs to different solids or fluid.

Processing

The solver *chtMultiRegionFoam* which is a combination of two others (heatConductionFoam and buoyontFoam) was used to solve the Navier-Stokes equation in the compressible form with the effects of gravity. Each region (solid and fluid) was solved separately and the data from each was used as boundary condition in the other region.

Post Processing

The main tool of OpenFOAM post processing is a reading module to be executed by the program Paraview [7], which is based in VTK, to process data and render images.

NusseltCalc [8] is another tool used to calculate the average value of the Nusselt number. *NusseltCalc* should be compiled in the operational system before use because it is not included in OpenFOAM.

EXPERIMENTAL ASSEMBLY

The experimental apparatus illustrated in Figure 3a was developed to conduct the tests. The heat sink was assembled on a resistive heater and both placed on a wood support as shown in Figure 3b. This assembly reduces heat loss through the bottom surface of the heater and does not restrict the air flow around the peripheral fins, Figure 3c. The sidewalls of the support were isolated with glass wool to prevent heat exchange between the support and the heat sink. Additionally, a medium density fiberboard was used to isolate the bottom of the heater to avoid buckling and to keep it in contact with the base of the heat sink. The thermocouples T4 and T5 were fixed by capacitive discharge in the center of the heat sink, T4 on the top and T5 in the base of the central fin. Thermocouple T3 is inserted directly into the heater to reduce the thermal contact resistance, and T2 was used to measure the part of the heat lost by conduction by the MDF (medium density fiber).

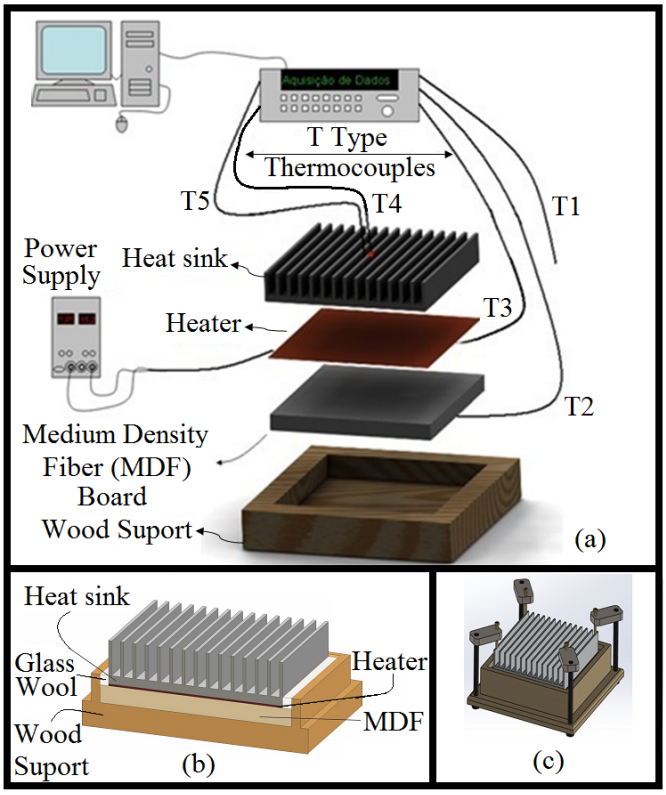

Figure 3 (a) Arrangement of test bench, (b) details of the heat sink, and (c) heat sink assemblies.

The heat sinks were machined from a single 6063-T5 aluminum bar to ensure high thermal conductivity [4]. Figure 1 and Table 2 show the geometric parameters values that made each heat sink different and unique. All these heat sinks were used for experimental tests, but only Heat Sinks 1 and 2 were used for simulations.

Table 2 – Dimensions of the Heat sinks**.**

	S [mm]	t [mm]	H [mm]	L [mm]	W [mm]	b [mm]	n	A_{ct} [m²]
Heatsink	Fin Spacing	Thickness	Height	Length	Width	Base Plate Thickness	Number of Fins	Total Area of Convection
H1	14.35	2.00	14.00	100.00	100.10	4.00	7	0.03
H2	5.55	2.00	14.00	100.00	100.15	4.00	14	0.05

RESULTS

All the cases were simulated in a computer with a 3.40 GHz CPU and 16.0 GB RAM memory through a virtual machine with a UBUNTU 64 bits operational system. It was also observed that the closed domain did not affect the heat exchange between the heat sink and fluid once the recirculation formed returns to the heat sink with the initial temperature.

For each case analysed, the same temperatures values used in Silva et al. [4] were adopted in the simulation.

Table 3 – Temperature values used in the simulations.

	CASE	T_1 [K]	T_5 [K]	ΔT [K]
Heat sink 1	A	295.94	304.30	8.36
	B	296.29	310.92	14.63
	C	295.63	322.07	26.44
	D	297.16	348.32	51.16
	E	295.45	369.26	73.81
Heat sink 2	F	296.84	304.92	8.09
	G	294.77	319.45	24.68
	H	293.55	330.27	36.72
	I	295.68	343.59	47.91
	J	296.07	363.28	67.22

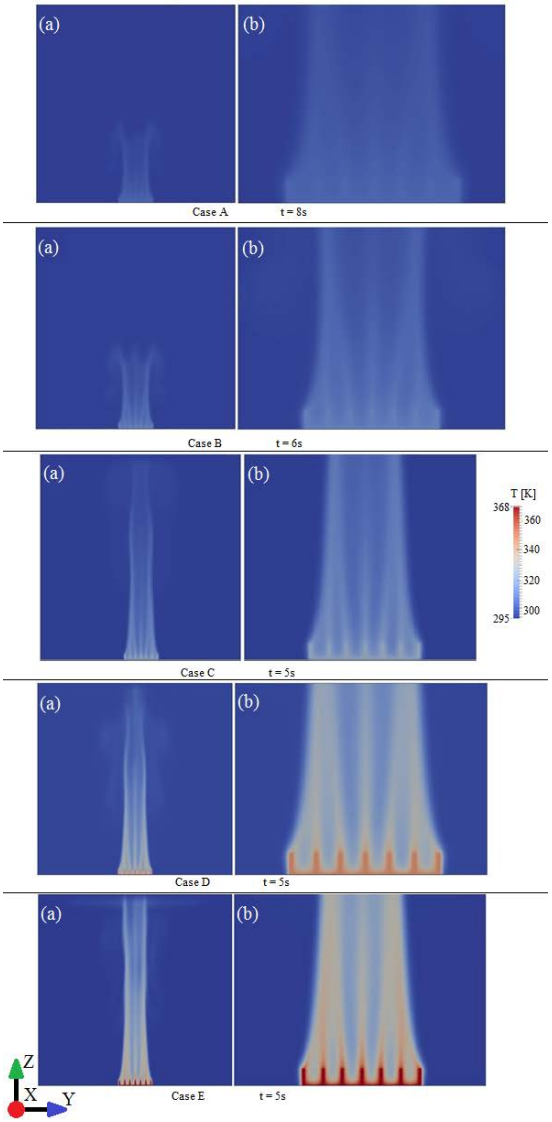

Figure 4 Temperature fields for each case of Heat sink 1, (a) sectional view and (b) enlarged view.

Temperature Fields

The upward flows of natural convection generated by the heating of Heat sink 1 base are shown in Figure 4. The heat is conducted to the whole heat sink and exchanged with the fluid. Thus a variation in the specific mass of the fluid appears resulting in different magnitudes of the buoyancy force, forming upward flow structures. Figure 4 shows the temperature field. Figure 4a presents the entire domain and Figure 4b a closer view. For these cases, the images were built in different times, because it was the moment in which they achieved the steady state.

Figure 4 shows the uniformity and symmetry of the temperature fields in the domain. The fluid temperature is high near the heat sink and it decreases as it moves away from the heat sink. It may be noted that the higher the temperature of the heat sink, the larger the area of the domain that suffers temperature increase. Figure 4 shows that the higher the temperature on the base of the heat sink the greater the temperature gradient on the fluid. This happens due to the low thermal conductivity of the air.

In order to validate the numerical results, Table 4 presents a comparison between the experimental, numerical and analytical temperatures of the top of the fin after the steady state was reached.

Table 4 – Experimental, numerical and analytical temperatures**.**

	CASE	T_4 experimental [K]	T_4 numeric [K]	T_4 analitical [K]	Deviation [%]
Heat sink 1	A	303,86	304,24	304,28	0,13
	B	310,03	310,82	310,89	0,25
	C	320,96	321,85	322,00	0,28
	D	347,39	347,91	348,14	0,15
	E	366,97	368,64	368,97	0,45
Heat sink 2	F	303,38	304,92	304,91	0,51
	G	320,02	319,44	319,41	0,18
	H	331,38	330,25	330,19	0,34
	I	342,47	343,56	343,49	0,32
	J	360,86	363,24	363,12	0,66

The percent deviations are lower than 0.7% between the numerical and experimental temperatures and it is observed that the analytical and numerical temperatures are close to the experimental temperatures.

A comparison between Heat sink 1 and 2 can be done by analysing Figure 5 where a couple of images shows the temperature fields for cases D and I (Table 3). These results were chosen due to their approximate power supply values.

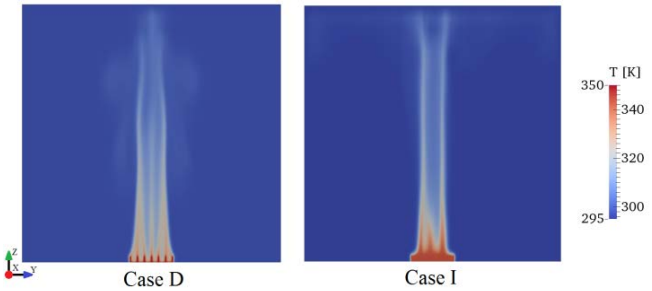

Figure 5 Visual comparison between Case D and Case I.

The differences between the temperature profiles of the fluid on the heat sinks may be observed in Figure 5. Case I has a more uniform profile in the domain and higher temperatures of the air near the heat sink. In Case D, the temperature profile has more curves over the heat sink which may suggest recirculation.

Velocity, Vorticity and Specific Mass fields

These fields are resultant of the heating of the air during the heat exchange with the heat sink. To show this phenomenon, Case D was chosen to illustrate what happens (Figure 6).

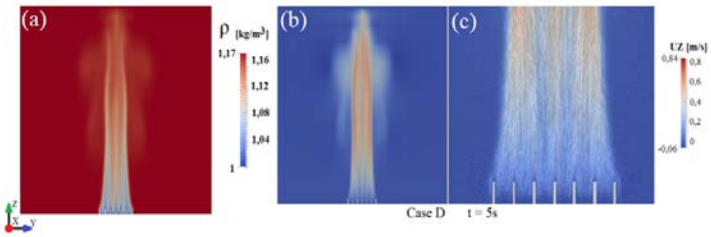

Figure 6 Specific mass field (a) and sectional view (b) and enlarged view (c) of velocity field for Case D.

There is a decrease of 15% in the specific mass in the area between fins, what made the air ascend in this region. This difference in the specific mass is larger for higher temperatures. Therefore, the higher the velocity of the air towards Z is.

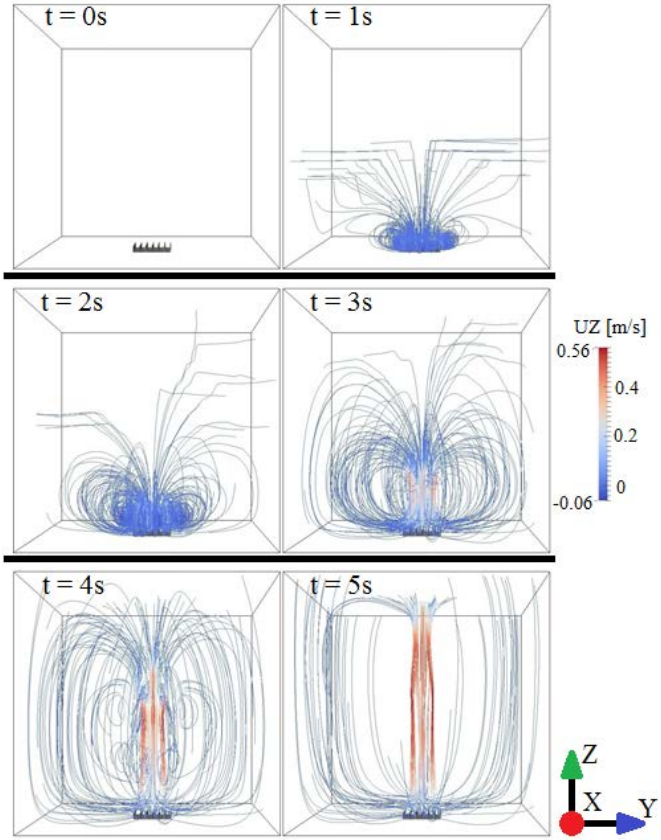

Figure 7 Temporal evolution of the streamlines for Case D.

Figure 7 shows the beginning of the simulation when it is possible to observe the formation of recirculation near the heat sink. The recirculation disappears as time progresses and a new recirculation that involves the entire domain rises until it reaches the steady state.

Figure 8 shows the vorticity field. Due the presence of the heat sink, it shows pairs of positive and negative signals, which indicate the way that the fluid tends to rotate. Figure 8 also shows secondary vortices in the edges of the fins and primary vortices in the edges of the heat sink as well as the propagation of this vorticity in Z direction.

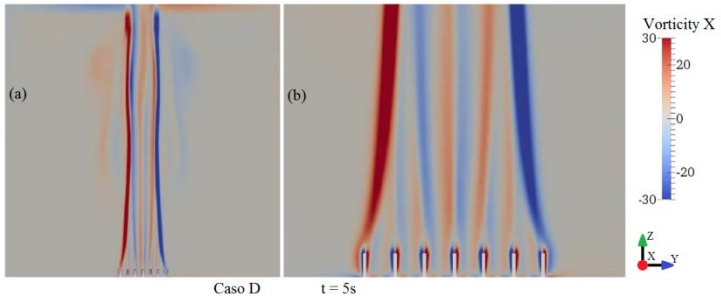

Figure 8 Vorticity fields for Case D.

Figure 9 presents the comparison of the cases for the values of $\bar{h}$ and Nusselt number for Heat sinks 1 and 2. The values obtained numerically and experimentally are close to literature values [6].

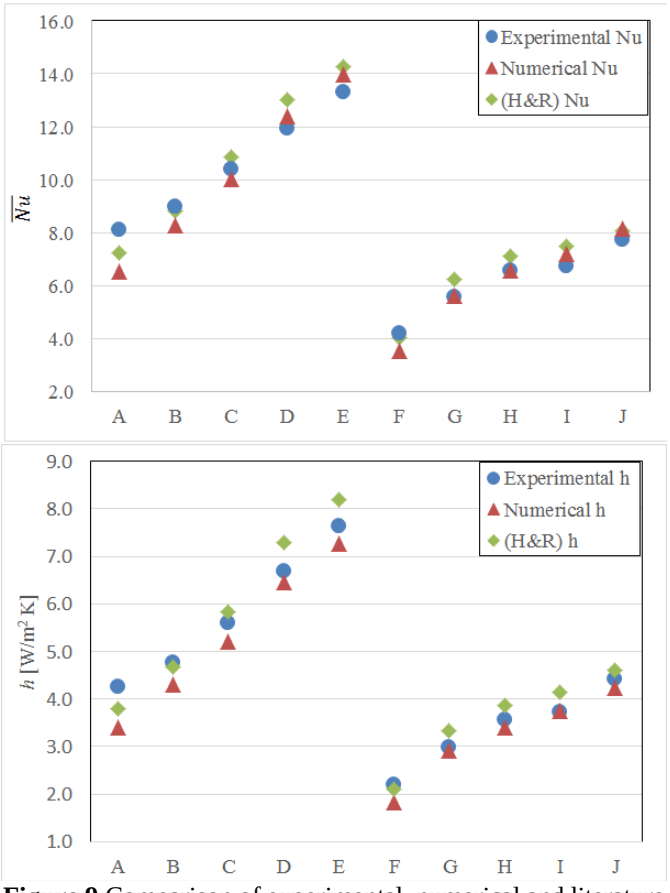

Figure 9 Comparison of experimental, numerical and literature results of Nusselt number and $\bar{h}$ for Heat sinks 1 and 2.

It is evident that Heat sink 1 has greater values for $\bar{h}$ and Nusselt number which means that the energy transferred to

the fluid is higher for this case. Heat sink 2 has lower temperatures as shown in Table 4 due to the combined effects of the convection and conduction that occurs in Heat sink 2. So it may be concluded that the combined effects between the convection and conduction are higher in Heat sink 2, even with lower values of $\bar{h}$ and Nusselt number.

The fields of local Nusselt number for cases D (Heat sink 1) and I (Heat sink 2) are shown in Figure 10.

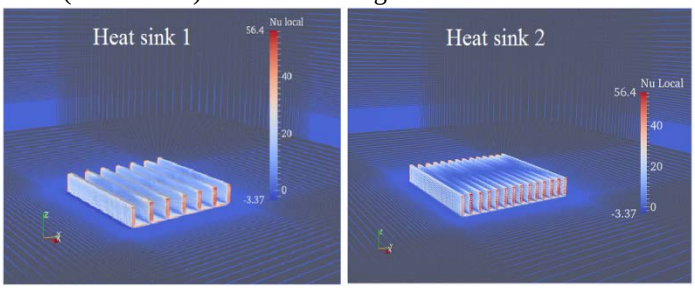

Figure 10 Field of Nusselt Number to Heat sink 1 (Case D) and Heat sink 2 (Case I).

Nusselt number values are higher in the border of the fins close to the spaces where the difference of temperature between the heat sink and the fluid is higher. Consequently, the values of heat exchange by convection and $\bar{h}$ are higher in the red region in Figure 10.

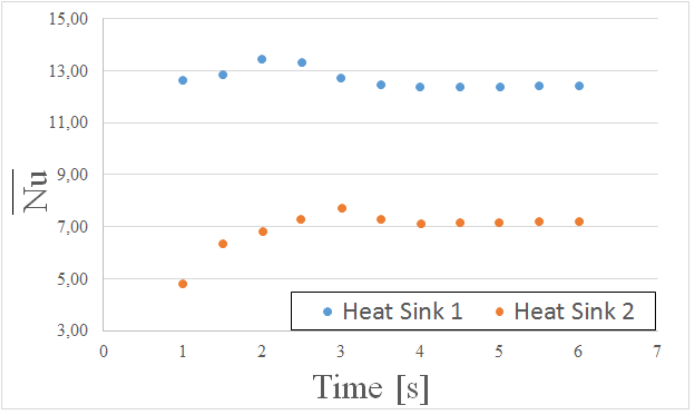

Figure 11 Temporal evolution of the average Nusselt number for Heat sink 1 and 2 in Case D.

Figure 11 shows that after 4 seconds of simulation the average Nusselt number becomes constant, what proves one more time that the steady state was reached. Other interesting analysis observed is that the two curves have similar behaviours.

CONCLUSION

The thermal and velocity fields showed a tendency of raising the fluid, after being heated around the heat sink. In addition, the propagation of the heat is consistent with the movement of the fluid. The recirculation of air in the heat sink, caused by the use of a closed domain, had little influence on the temperature values, since they showed good agreement with average deviations, lower than 0.7%, with experimental and analytical temperature values.

The numerical values of the Nusselt number also showed good agreement when compared with the experimental values and the values obtained by the empirical correlation of Harahap and Rudianto [6,9]. The numerical values of $\bar{h}$ also approached the experimental values with an average deviation lower than 8%. When compared to the correlation values, it showed a mean deviation lower than 10%. Noteworthy is the fact that the numerical and experimental values of $\bar{h}$ were closer for the cases with higher temperatures with the lowest deviation of less than 0,6%

The OpenFOAM software proved to be a reliable tool in the study of heat transfer problems and stands out as an important research tool since it is free and open sourced.

ACKNOWLEDGEMENTS

The authors would like to thank CNPq, FAPEMIG (Processes APQ-0334-14 and APQ-02850-14) and CAPES for their financial support.

REFERENCES

[1] Ledezma, G. and Bejan, A., Heat sinks with sloped plate fins in natural and forced convection, *Int. J. of Heat and Mass Transfer*, vol. 39, 1996, pp. 1773-1783.

[2] Jouhara, H. and Axcell, B.P., Modelling and simulation techniques for forced convection heat transfer in heat sinks with rectangular fins, *Simulation Modelling Practice and Theory*, vol. 17, 2009, pp. 871-882.

[3] Silva, V.A., Anselmo, B.C.S., Lima e Silva, A.L.F. and Lima e Silva S.M.M., Experimental analysis of the influence of heat sink geometric parameters on natural convection, *23rd ABCM International Congress of Mechanical Engineering, COBEM 2015*, Rio de Janeiro, Brazil, December 2015.

[4] Silva, V.A., *Experimental analysis of the influence of heat sink geometric parameters convection*, Itajubá, 100p. MSc. Dissertation (in Portuguese), Programa de Pós-graduação em Engenharia Mecânica, Universidade Federal de Itajubá, 2015.

[5] Tari, I. and Mehrtash, M., Natural convection heat transfer from inclined plate-fin heat sinks, *Int. J. of Heat and Mass Transfer*, vol. 56, 2012, pp. 574-593.

[6] Harahap, F. and Rudianto, E., Measurements of steady-state heat dissipation from miniaturized horizontally based straight rectangular fin arrays, *Heat and Mass Transfer*, vol.41, 2005, pp. 280-288.

[7] Ahrens, J., Geveci, B. and Law C., *ParaView: an end-user tool for large data visualization"*, *Visualization Handbook*, Elsevier.

[8] Magnussom, J., *ConjugateHeatFoam with explanational tutorial together with a buoyancy driven flow tutorial and a convective conductive tutorial*, Magnusson's Technology Center, Chalmers University of Technology, Gothenburg, Sweden, 42p, 2010.

[9] Harahap, F. and Rudianto, E., Measurements of steady-state heat dissipation from miniaturized horizontally-based straight rectangular fin arrays, Erratum, *Heat and Mass Transfer*, vol.41, 2005, pp. 289-289.